ORIGINAL RESEARCH

Beneficial Effect of Renal Denervation on Ventricular Premature Complex Induced Cardiomyopathy

Shinya Yamada, MD; Li-Wei Lo, MD; Yu-Hui Chou, MS; Wei-Lun Lin, MS; Shih-Lin Chang, MD; Yenn-Jiang Lin, MD; Shin-Huei Liu, MD; Wen-Han Cheng, MD; Tsung-Ying Tsai, MD; Shih-Ann Chen, MD

***Background*—**Frequent ventricular premature complexes (VPCs) can lead to the development of dilated cardiomyopathy and sudden cardiac death. Renal artery sympathetic denervation (RDN) may protect the heart from remodeling. This study aimed to investigate the effect of frequent VPCs on structural and electrical properties and whether RDN can protect the heart from remodeling.

***Methods and Results*—**Eighteen rabbits were randomized to control (n=6), VPC (n=6), and VPC-RDN (n=6) groups. Surgical and chemical RDNs were approached through bilateral retroperitoneal flank incisions in the VPC-RDN group. Pacemakers were implanted to the left ventricular apex to produce 50% VPC burden for 5 weeks in the VPC and VPC-RDN groups. In addition, ventricular myocardium was harvested for western blot and trichrome stain. Echocardiographic results showed left ventricular enlargement after 5-week pacing in the VPC group, but not in the VPC-RDN group, when compared to baseline. In biventricles, ion channel protein expressions of Nav1.5, Cav1.2, Kir2.1, and SERCA2 were similar among 3 groups. However, the degree of biventricular fibrosis was extensive in the VPC group, compared to the control and VPC-RDN groups. Importantly, ventricular fibrillation inducibility was higher in the VPC group (41%) when comparing to the control (13%; $P<0.05$) and VPC-RDN groups (13%; $P<0.05$), respectively.

***Conclusions*—**Frequent VPCs are associated with the development of cardiac structural remodeling and high ventricular fibrillation inducibility. RDN prevents cardiac remodeling and the occurrence of ventricular arrhythmia through antifibrosis. **(*J Am Heart Assoc*. 2017;6:e004479. DOI: 10.1161/JAHA.116.004479.)**

Key Words: antifibrosis • remodeling • renal denervation • ventricular arrhythmia

Ventricular premature complexes (VPCs) are common findings on electrocardiography in general population, which are often regarded as benign.[1,2] However, trigger VPCs with a short coupling interval may carry the risk of initiating ventricular fibrillation (VF) and sudden cardiac death.[3] In addition, increased VPC burden can cause dilated cardiomyopathy with left ventricular (LV) dysfunction.[4,5] It has been generally described that VPC-induced cardiomyopathy could be reversible and appears to be a functional abnormality in human and animal models.[6–8] However, it has been shown that there are some patients with partial improvement of LV function despite the elimination of VPCs,[9] and frequent VPCs in animal model leads to an increase in interstitial fibrosis.[5] Therefore, the mechanism of the development of VPC-induced cardiomyopathy and its histological and electrophysiological characteristics have not been fully clarified.

Renal artery sympathetic denervation (RDN) has been demonstrated to attenuate sympathetic outflow through the brain to the heart as well as decreasing systemic catecholamine excretion.[10] Although the Symplicity HTN-3 trial failed to demonstrate a beneficial result of RDN in the patients with resistant hypertension,[11] RDN may have great potential in the treatment of other cardiovascular diseases, such as heart failure,[12] atrial fibrillation,[13] and ventricular tachyarrhythmias,[14] beyond the changes of blood pressure. It is also possible that RDN is effective for preventing the development of atrial and ventricular remodeling because RDN could suppress the activity of the renin-angiotensin-aldosterone system and inflammatory cytokines.[15] Thus, this study aimed to investigate the effect of frequent VPCs on structural and electrical remodeling and whether RDN can protect the heart from remodeling.

From the Division of Cardiology, Department of Medicine, Taipei Veterans General Hospital, Taipei City, Taiwan, R.O.C. (S.Y., L.-W.L., Y.-H.C., W.-L.L., S.-L.C., Y.-J.L., S.-H.L., W.-H.C., T.-Y.T., S.-A.C.); Department of Cardiovascular Medicine, Fukushima Medical University, Fukushima, Japan (S.Y.); Institute of Clinical Medicine, and Cardiovascular Research Institute, National Yang-Ming University, Taipei, Taiwan (L.-W.L., W.-L.L., S.-L.C., Y.-J.L., S.-H.L., W.-H.C., T.-Y.T., S.-A.C.).

Correspondence to: Shih-Ann Chen, MD, Division of Cardiology, Taipei Veterans General Hospital, No. 201, Sec. 2, Shipai Rd, Beitou District, Taipei City, 11217 Taiwan, R.O.C. E-mail: epsachen@ms41.hinet.net and Li-Wei Lo, MD, Division of Cardiology, Taipei Veterans General Hospital, No. 201, Sec. 2, Shipai Rd, Beitou District, Taipei City, 11217 Taiwan, R.O.C. E-mail: gyrus@ms65.hinet.net

Received August 12, 2016; accepted November 29, 2016.

Methods

Animal Preparation

The present study protocol was reviewed and approved by the Institutional Animal Care and Committee of Taipei Veterans General Hospital. All surgical procedures were performed under general anesthesia. After procedure, rabbits received antibiotics infusion (gentamicin, 5–8 mg/kg) and ibuprofen (2–10 mg/kg) in their water for 3 days for pain relief. All efforts were made to minimize suffering animals. A total of 18 male New Zealand white rabbits (weight 2.5–3.0 kg, from Shulin Breeding facility, New Taipei, Taiwan) at 12 weeks of age were used. One animal per cage was housed in a temperature-regulated room with a 12:12-hour light-dark cycle and unlimited access to food and water.

Pacemaker Implantation and Pacing Protocol

In brief, an intramuscular injection of a mixture of Zoletil 50 (10 mg/kg) and xylazine (5 mg/kg) was given at the beginning of the procedure. Repeated injections of Zoletil 50 and xylazine were administered as required to maintain a deep level of anesthesia. An intravenous catheter was inserted into the marginal ear vein for the anesthetics. Rabbits were then intubated and ventilated artificially with room air or supplemented with oxygen to maintain oxygen saturation >95%. After opening the left third intercostal space, part of the pericardium was cut to expose the anterior surface of the heart. Two unipolar pacing leads (pacing lead 6491; Medtronic, Ltd., Minneapolis, MN) fixed to the LV free wall was connected to the dual-chamber pacemaker, which was implanted subcutaneously at the left subaxillary area. One week after implantation of the pacemaker, pacemaker was programmed to the VDD mode in the rabbits of the VPC and VPC-RDN groups. Intrinsic ventricular depolarization were sensed by lead attached to the atrial port, and the pacing impulses were given from a second lead through the ventricular port. The mode allowed us to create the bigeminal pattern with 50% of VPC burden in both the VPC and VPC-RDN groups. The atrioventricular delay was set as 50 ms longer than the ventricular effective refractory period (ERP). The electrocardiogram was checked weekly to confirm the effective pacing.

Rabbit RDN Model

By using the same anesthesia method, both kidneys were approached through mid-abdominal incision. The chemical RDN has been reported on before.[16] In brief, the rabbit underwent fasting for 1 night before the surgery. Bilateral kidneys were surgically denervated by cutting all visible nerves in the area of the renal hilus (surgical RDN) and by stripping ≈1 cm of the adventitia from the renal artery. The area was then moistened with a 20% phenol solution for 10 to 15 minutes (chemical RDN). Post-RDN, animals were allowed to re-equilibrate for 1 hour and the abdomen was closed layer by layer with suture and bleeding was checked. Figure 1 shows an example of how combined surgical and chemical RDNs were performed during the experiment.

Echocardiographic Study

We evaluated the cardiac function at baseline and the end of a 5-week pacing by an ultrasound system (MicroMaxx; SonoSite Inc., Bothell, WA). After the subcutaneous administration of ketamine (17 mg/kg) and xylocaine (7 mg/kg), sedated rabbits, having their anterior chest and upper abdomen hair removed, were placed in the right lateral decubitus position. LV size (LV end-diastolic diameter [LVEDD] and LV end-systolic diameter [LVESD]) was measured using the M mode in the parasternal short-axis view. LV ejection fraction (LVEF) was also measured using Teichholz formula. All measurements were obtained from 3 cardiac cycles and the data were averaged.

Biochemical Study

Blood samples were collected from the central auricular artery of the rabbits at baseline and the end of a 5-week pacing. Plasma was obtained by centrifuging the blood at 1710 g for 10 minutes at 4°C, and then the content of blood urea nitrogen (BUN), creatinine, and renin were examined.

Experimental Procedures

The rabbits were randomized to 3 groups:

1. Sham-operated control group (n=6): There was no pacemaker implantation nor RDN in the group.
2. VPC group (n=6): Rabbits received a left thoractomy with implantation of a pacemaker. After 1 week of recovery, LV apex pacing (50% VPC burden) was started and followed by observation for 5 weeks before the experiment.
3. VPC-RDN group (n=6): Rabbits received both a left thoractomy with pacemaker implantation and bilateral RDNs. After 1 week of recovery, LV apex pacing (50% VPC burden) was started and followed by observation for 5 weeks before the experiment.

General preparation

On the day of experiment, a warming blanket was used for rabbits to maintain body temperature. An intravenous line was set up for the medication and fluid supplement. All rabbits

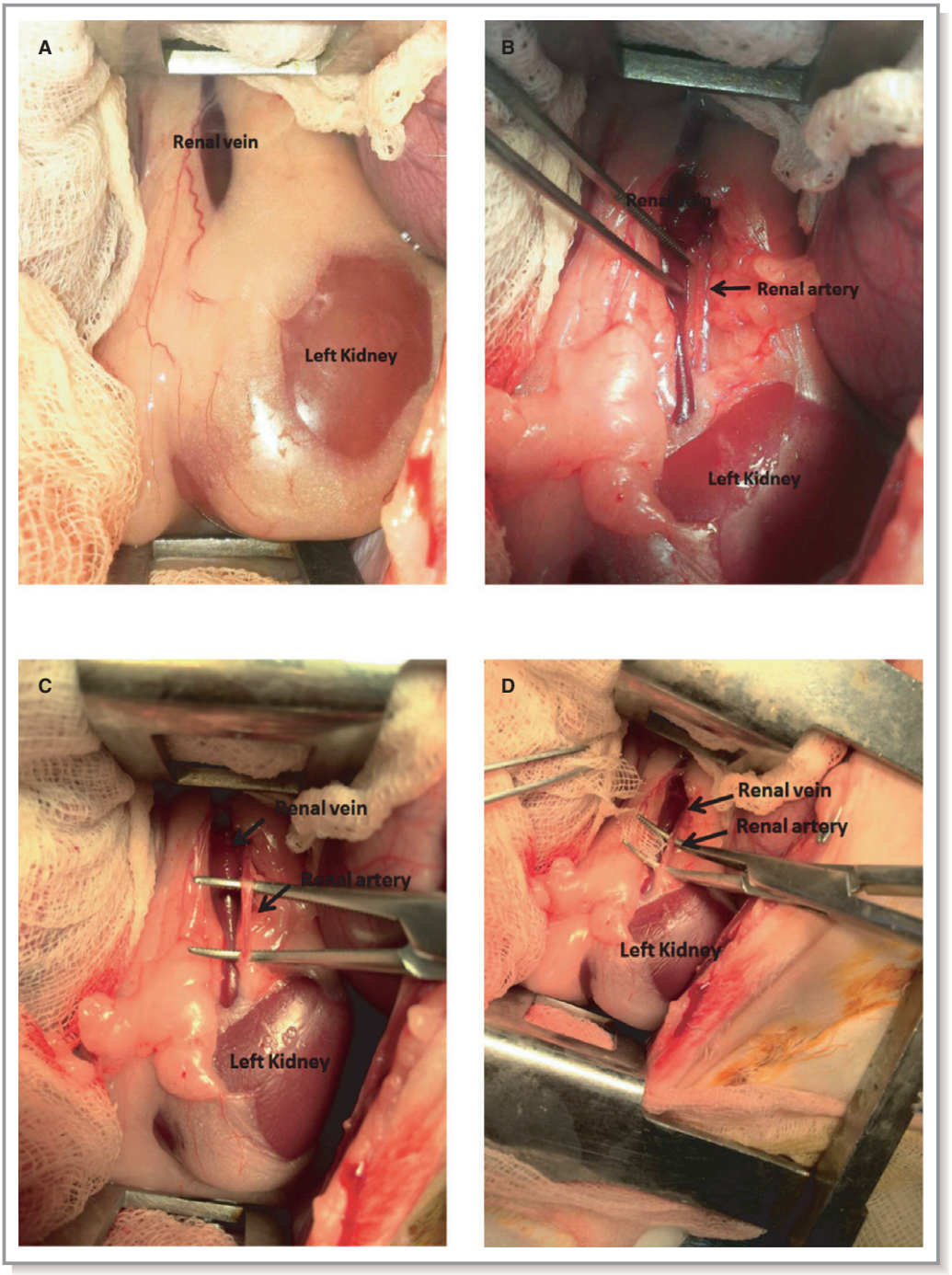

Figure 1. Renal artery sympathetic denervation procedure. Renal vessels were exposed (A) and renal artery is dissected (B) with removal of peripheral fat (C) and then application of gauge with phenol solution for 10 to 15 minutes (D).

were anesthetized with an intraperitoneal injection of sodium pentobarbital (40 mg/kg). They were artificially ventilated through a cuffed endotracheal tube by a constant volume-cycled respirator with room air or oxygen, as needed. The rabbit was put in the supine position. A mid-thoracotomy was performed and the muscle was dissected with carefully bleeding checkup in the procedure until the exposure of the mediastinal space. The pericardium was then incised to expose the whole heart completely.

Conventional electrophysiology study and induction of VF

In all rabbits, programmed electrical stimulation was performed by a custom-made stimulator (Model 5325;

Medtronic) that delivered constant-current pulses of 1-ms duration. Programmed electrical stimulation was delivered to the multielectrode catheter distal tips at 2 and 10 times the pacing threshold that sutured epicardially at biatria and -ventricle. Eight S1 to S1 300-ms cycles were followed by an extrastimlus. Decremental pacing by 10 and then 1 ms was maintained until the atrial ERP and the ventricular ERP were detected. The shortest S1 to S2 interval that results in a propagated atrial and ventricular response was taken as the atrial and ventricular ERPs, respectively. VF inducibility was defined as an incidence of sustained (>30 seconds) VF induced by shortest S1 to S1 pacing with maximum pacing threshold during 10 inductions. If the VF sustained for more than 0.5 minutes, an external electrical defibrillation was performed to restore to sinus rhythm.

Tissue harvest

Rabbits were sacrificed by exsanguination under anesthesia at the end of the electrophysiology study, and atrial and ventricular myocardium harvested from 3 groups were obtained. Atrial and ventricular tissues were sampled at the biatrial and -ventricular free walls and flushed free of blood. A fixation procedure was performed immediately in both 20% formalin and liquid nitrogen to prevent sample degradation. Renal sampling was also performed with kidneys frozen in liquid nitrogen and stored at −80°C to allow adrenaline and noradrenaline concentrations to be determined.

Western Blot Analysis

The myocardium sample of biventricle was homogenized and loaded onto 10% SDS/polyacrylamide gel. Proteins were transferred to nitrocellulose filters. Nitrocellulose filters were blocked with 5% albumin in TBS-T buffer for 30 minutes at room temperature. Membranes were subsequently exposed overnight to primary antibody in 2% albumin with TBS-T at 4°C. Excess primary antibodies were washed from the nitrocellulose membranes with three 10-minute washes in TBS-T, and then these membranes were incubated with the ECL anti-rabbit immunoglobulin G fragment in TBS-T. After 3 further 10-minute washes in TBS-T, bound antibodies were detected with the ECL Western Blotting Detection System (EMD Millipore, USA). In the present study, ionic channel proteins, including α-subunit of cardiac sodium channels (Nav1.5; Alomone Labs, Jerusalem, Israel) and cardiac calcium channels (CaV1.2; Thermo Scientific, Waltham, MA), inward-rectifier potassium ion channel (Kir2.1; Santa Cruz Biotechnology, Santa Cruz, CA), and SR-calcium-ATPase2 (SERCA2; Thermo Scientific) protein expressions, were analyzed. In all groups, CaV1.2, NaV1.5, and Kir2.1 proteins appeared as 240-, 250-, and 48-kDa single band, respectively. In addition, SERCA2 protein appeared as a 110-kDa single band.

Histological Study

Biatrial and -ventricular tissues were dehydrated by sequential washes with 70% ethanol, 80% ethanol, 90% ethanol, and 100% ethanol and then imbedded in the paraffin. Sections were cut parallel to the plane of atrioventricular annulus to include the epi- and endocardial aspects of the myocardium in each slice and dyed with Masson's trichrome, which resulted in fibrotic (collagen-enriched) areas appearing blue, whereas cellular elements appeared red. Masson's trichrome-stained myocardial sections were imaged, and the collagen areas of ventricle and atria were calculated as a percentage of the total ventricular and atrial myocardial areas with an image analyzer (Image-Pro Plus 6.0; Media Cybernetics, Inc., Rockville, MD), respectively. This result served as an estimate of progression of fibrosis. For the immunohistochemistry staining, antibodies for tyrosine hydroxylase (TH) were used to stain sympathetic nerves. Sympathetic neuron marker densities were measured as total area of nerves (μm^2) per square millimeter with an image analyzer (Image-Pro Plus 6.0; Media Cybernetics).

Statistical Analysis

Normally distributed data were reported as mean values±SE. Other not normally distributed data were reported as median and interquartile range (IQR). Categorical data are presented as absolute values and percentages. Data variables among the groups (intergroup) were compared with the Kruskal–Wallis test, and if P was <0.05, follow-up comparisons of the different groups were done with Dunn's test. In normally distributed data, an independent-sample t test was used to analyze the differences between VPC rabbits and VPC-RDN rabbits and a paired-sample t test was used to evaluate whether there were differences before and after pacing. In addition, we used a Wilcoxon signed-rank test to evaluate whether there were differences in LVEF, LVEDD, and LVESD before and after pacing. $P<0.05$ was deemed statistically significant. Analysis was performed by a senior biostatistician using SPSS statistical software (Version 22.0; SPSS Institute, Inc., Chicago, IL).

Results

Echocardiographic Data

Figure 2 shows LVEF, LVEDD, and LVESD from echocardiographic examination at baseline and the end of a 5-week pacing. In VPC rabbits, LVEF after pacing (median, 34.7%; IQR, 23.7–65.8) tended to decrease compared to baseline (median, 72.3%; IQR, 64.0–85.1). LVEDD and LVESD after pacing were significantly greater than those of baseline (LVEDD: median, 11.5 mm; IQR, 10.3–15.0 vs median, 9.2 mm; IQR,

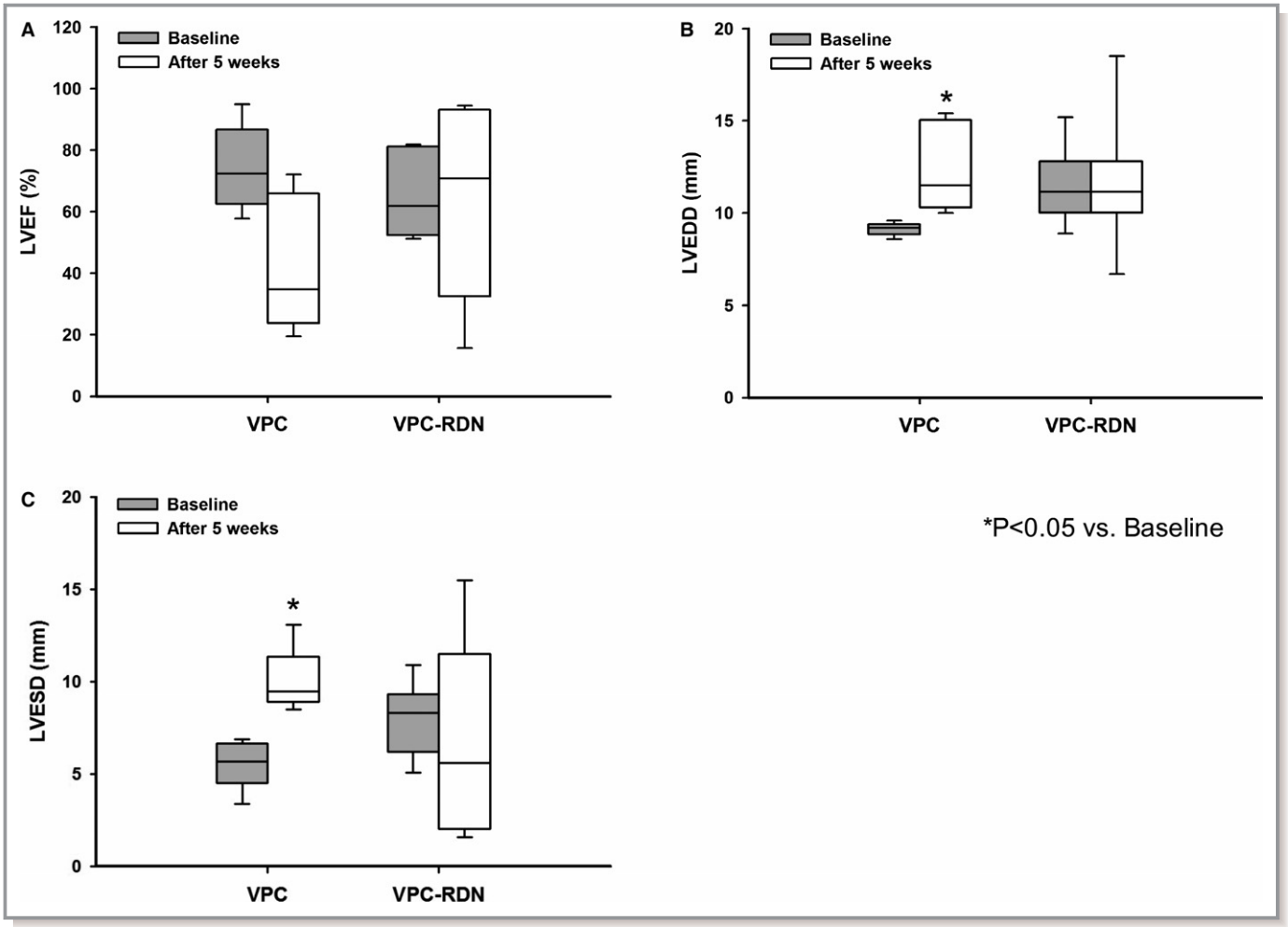

Figure 2. Left ventricular function from echocardiographic examination during a 5-week follow-up. A, LVEF at baseline and the end of a 5-week pacing in VPC rabbits and VPC-RDN rabbits. B, LVEDD at baseline and the end of a 5-week pacing in VPC rabbits and VPC-RDN rabbits. C, LVESD at baseline and the end of a 5-week pacing in VPC rabbits and VPC-RDN rabbits. LVEDD indicates left ventricular end-diastolic diameter; LVEF, left ventricular ejection fraction; LVESD, left ventricular end-systolic diameter; RDN, renal artery sympathetic denervation; VPC, ventricular premature complex.

8.8–9.4; LVESD: median, 9.5 mm; IQR, 8.9–11.3 vs median, 5.7 mm; IQR, 4.5–6.6; $P<0.05$), respectively. On the other hand, there were no significant differences in LVEF, LVEDD, and LVESD of VPC-RDN rabbits between baseline and after pacing, respectively.

Biochemical Characteristics

There were no significant differences in renin, BUN, and creatinine at baseline between VPC rabbits and VPC-RDN rabbits. In VPC rabbits, renin after pacing was significantly higher than that of baseline (0.70±0.16 vs 0.28±0.07 pg/mL; $P<0.05$). However, there were no significant differences in BUN and creatinine (BUN, 13.2±2.9 vs 11.5±0.8 mg/dL; creatinine, 0.89±0.13 vs 0.93±0.07 mg/dL), respectively. In VPC-RDN rabbits, there were no significant differences in renin, BUN, and creatinine between baseline and after pacing (renin, 0.43±0.16 vs 0.56±0.19 pg/mL; BUN, 13.4±2.6 vs 10.8±1.3 mg/dL; creatinine, 1.00±0.16 vs 0.93±0.13 mg/dL), respectively.

Effective Refractory Period and Induction of VF After RDN

Table 1 shows ERPs among 3 groups in biventricles and -atria, respectively. There were no significant differences in biventricular ERPs between control and VPC rabbits, respectively. However, biventricular ERPs of VPC-RDN rabbits were significantly longer compared with those of control rabbits, respectively. There were no significant differences in biatrial ERPs among 3 groups. Sustained VF could be induced and VF inducibility was higher in VPC rabbits (41%), when compared

Table 1. Comparisons of Effective Refractory Periods

Groups	Control	VPC	VPC-RDN
Right ventricular ERP, ms			
Two times the pacing threshold	141 (136–158)	169 (160–177)	190 (174–217)*
Ten times the pacing threshold	111 (89–117)	135 (125–139)	168 (150–184)*
Left ventricular ERP, ms			
Two times the pacing threshold	149 (135–160)	172 (149–201)	179 (165–213)*
Ten times the pacing threshold	123 (113–137)	139 (130–156)	170 (144–189)*
Right atrial ERP, ms			
Two times the pacing threshold	69 (58–84)	79 (62–89)	82 (78–86)
Ten times the pacing threshold	64 (53–69)	62 (59–66)	62 (59–65)
Left atrial ERP, ms			
Two times the pacing threshold	69 (59–89)	82 (78–101)	91 (76–114)
Ten times the pacing threshold	60 (48–89)	79 (67–102)	86 (73–101)

Data are presented as median (interquartile range). ERP indicates effective refractory periods; RDN, renal artery sympathetic denervation; VPC, ventricular premature complex.
*P<0.05 (control vs VPC-RDN).

to control (13%; P<0.05) and VPC-RDN rabbits (13%; P<0.05), respectively.

Kidney Tissue Catecholamine After RDN

Table 2 shows the detail of the renal catecholamine levels. Both norepinephrine and adrenaline contents of renal tissue extracts were significantly lower in VPC-RDN rabbits than those of control and VPC rabbits, respectively. There were no significant differences in renal catecholamine levels between VPC rabbits and control rabbits.

Ionic Channel Proteins in the Ventricle After RDN

In both right and left ventricles, ion channel protein expressions of NaV1.5, CaV1.2, Kir2.1, and SERCA2 were similar among 3 groups, as shown in Figure 3.

Tissue Fibrosis in the Ventricle and the Atrium After RDN

To assess the progression of the fibrosis, both biventricular and -atrial tissues were evaluated with Masson's trichrome staining, as shown in Figures 4 and 5. Degree of biventricular fibrosis was extensive in VPC rabbits compared to those of control and VPC-RDN rabbits, respectively (see Figure 4). Degree of biatrial fibrosis was also extensive in VPC rabbits compared to those of control and VPC-RDN rabbits, respectively.

Immunohistochemistry Staining

Figure 6 illustrates examples of the histological studies from the myocardium with TH staining in control (Figure 6A and 6D), VPC (Figure 6B and 6E), and VPC-RDN (Figure 6C and 6F) rabbits. Sympathetic neuron marker densities in biventricle were significantly higher in VPC rabbits compared with those of control and VPC-RDN rabbits, respectively (Figure 7).

Discussion

The main findings of this study are: (1) Progressive ventricular chamber dilatation was noted in VPC rabbits and the degree of biventricular fibrosis in VPC rabbits was extensive compared to those of control rabbits; (2) VF inducibility was

Table 2. Comparisons of Renal Catecholmine Levels Measured Among 3 Groups During the Experiment

Groups	Control (n=6)	VPC (n=6)	VPC-RDN (n=6)
Noradrenaline level, ng/mL	5.30 (5.14–5.46)	4.57 (4.00–5.39)*	1.00 (0.63–1.25)†
Adrenaline level, ng/mL	0.58 (0.50–0.69)	0.41 (0.30–0.56)‡	0.27 (0.10–0.36)†

Data are presented as median (interquartile range). ERP indicates effective refractory periods; RDN, renal artery sympathetic denervation; VPC, ventricular premature complex.
*P<0.01 versus VPC-RDN rabbits.
†P<0.01 versus control rabbits.
‡P<0.05 versus VPC-RDN rabbits.

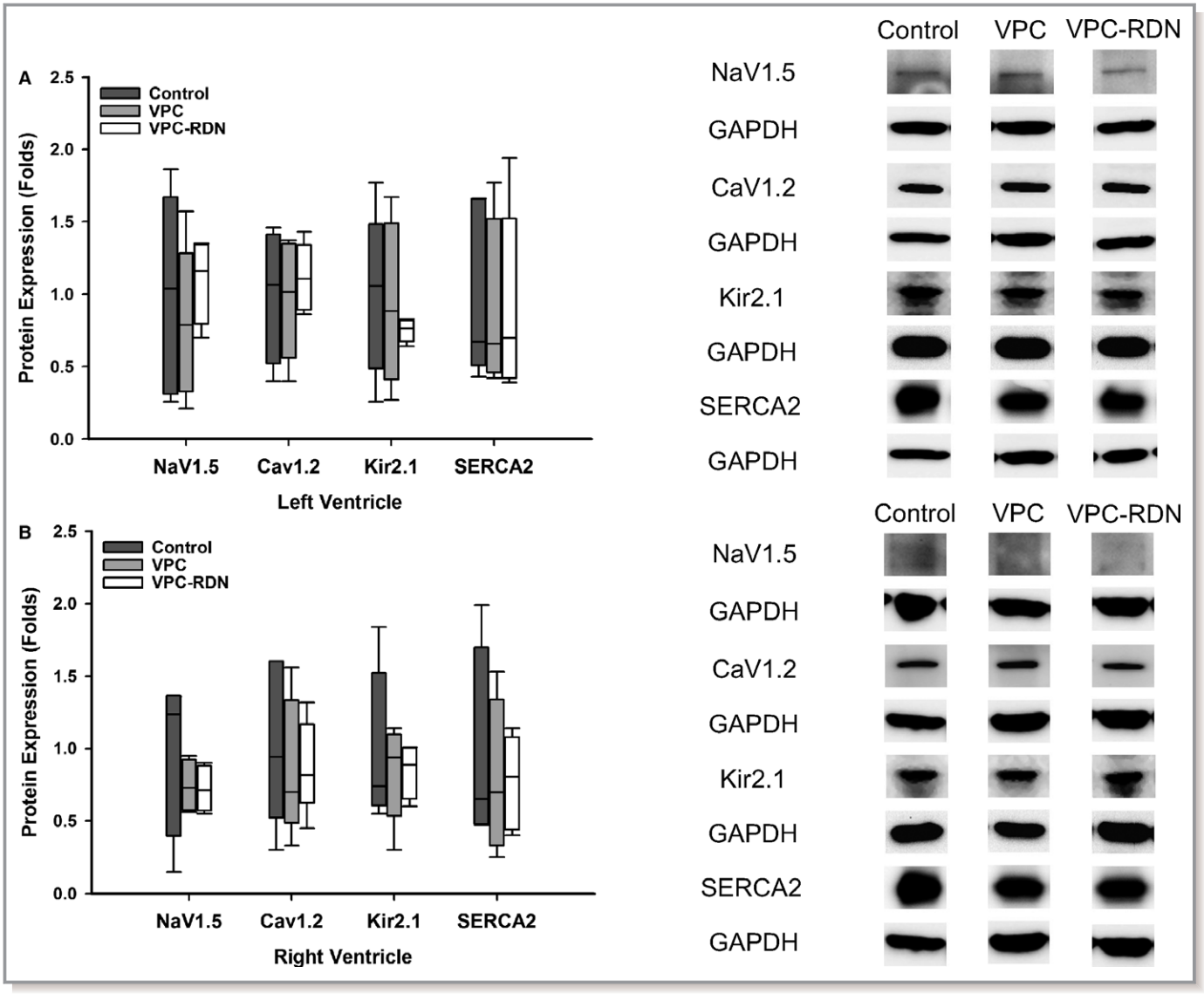

Figure 3. Ion channel protein expressions of NaV1.5, CaV1.2, Kir2.1, and SERCA2 in right ventricle (RV) and left ventricle (LV). A, Protein expression of NaV1.5, CaV1.2, Kir2.1, and SERCA2 among 3 groups in LV (left panel). Right panel shows the representative western blots of the protein sample extracts from the LV. B, Protein expression of NaV1.5, CaV1.2, Kir2.1, and SERCA2 among 3 groups in RV (left panel). Right panel shows the representative western blots of the protein sample extracts from the RV. RDN indicates renal artery sympathetic denervation; VPC, ventricular premature complex.

significantly higher in VPC rabbits compared to those of control and VPC rabbits; (3) ERPs, ionic channel protein expressions, and renal catecholamine levels were not different between VPC rabbits and control rabbits; and (4) ventricular chamber dilatation was not noted in VPC-RDN rabbits and extent of biventricular fibrosis in VPC-RDN rabbits was significantly decreased by RDN compared to those of VPC rabbits. Therefore, our study findings indicated that frequent VPCs may cause ventricular structural remodeling, resulting in an increase of VF inducibility. RDN can regulate the ventricular arrhythmogenic substrates and suppress VF inducibility, mostly through reverse structural remodeling.

Frequent VPCs and Ventricular Structural Change

Some studies showed that frequent VPCs lead to dilated cardiomyopathy with LV dysfunction.[4,5] In swine models with 50% pacing burden during a 14-week follow-up, there were progressive increase in LVEDD and LVESD and decrease in LVEF without signs of overt heart failure, such as lethargy, decreased activity, fluid retention, or tachypnea.[5] In our models with 50% VPC burden during a 5-week follow-up, there was a progressive chamber dilatation without signs of overt heart failure. In addition, VPC rabbits showed similar renal catecholamine levels compared to control rabbits. Although the average LVEF after 5-week pacing was lower compared to

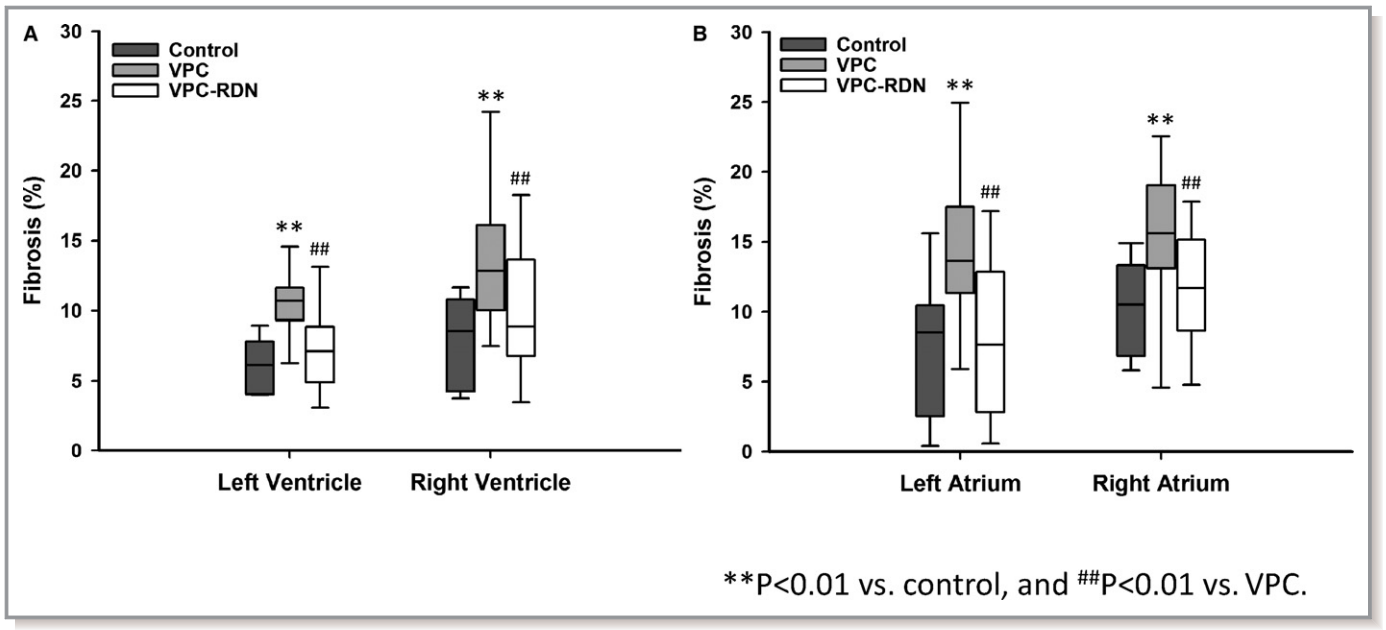

Figure 4. Quantitative analysis of fibrotic area in the ventricle and atrium among all groups. The collagen area was calculated as a percentage of the total ventricular or atrial myocardial area. A, Trichrome stain results of the left and right ventricle. B, Trichrome stain results of the left and right atrium. RDN indicates renal artery sympathetic denervation; VPC, ventricular premature complex.

the baseline, the difference did not reach a statistically significant level. One possible reason for this result is that the duration of pacing exposure in our study was shorter compared to animals in previous studies.[4,5] Second, different animal species may have a different vulnerability to cardiomyopathy secondary to VPC.

Effect of RDN on Cardiac Remodeling

Histological and electrophysiological characteristics of the dilated cardiomyopathy induced by VPCs has not been fully elucidated. Several studies have reported that the elimination of VPCs by radiofrequency catheter ablation can improve LV structure and function.[6,7] However, there are some patients with partial improvement LV function or persistent LV dilation despite the elimination of VPCs.[9] Those findings might suggest that some patients have residual structural changes. In our study, VPC rabbits demonstrated increases in biventricular and -atrial myocardial fibrosis compared to those of control rabbits, but the degree of fibrosis was dramatically suppressed in VPC-RDN rabbits. These results showed that frequent VPCs developed ventricular and atrial structural remodeling, but RDN had beneficial effects on preventing structural remodeling.

Sympathetic nerve stimulation is considered to decrease ventricular ERP and action potential duration.[17,18] It has been reported that RDN prolonged ventricular ERP and action potential duration, and reduced the dispersion of ventricular ERP and slope of the restitution curve because RDN might decrease the sympathetic effects on the heart.[19] Ventricular ERPs of VPC rabbits were not different compared to those of control rabbits, but ventricular ERPs of VPC-RDN rabbits were significantly longer than those of control rabbits. In the present study, decreased catecholamine levels of VPC-RDN rabbits might be associated with ventricular ERP prolongation.

In order to evaluate the ventricular ionic remodeling, we analyzed ionic channel proteins, including NaV1.5, CaV1.2, Kir2.1, and SERCA2 protein expressions. Although the detailed roles of potassium, sodium, and calcium currents and channels in heart failure still remain unclear, a reduced inward rectifier potassium current[20] and an increased late component of sodium current[21] may contribute to prolongation of action potential duration. In addition, some studies showed that altered calcium homeostasis, including reduced inward L-type calcium current and SERCA function, may induce contractile dysfunction, resulting in the progression of heart failure and arrhythmogenicity with electrical remodeling.[22–24] In VPC-induced cardiomyopathy models without heart failure, a recent study reported that frequent VPCs reduced inward L-type Ca current density, but the difference of Cav1.2 protein did not reach a statistically significant level compared to control.[25] In their study, Kir2.1 protein levels also did not differ statistically. In the present study, we also have the similar finding that Cav1.2 and Kir2.1 protein levels of control and VPC rabbits were comparable. In addition, NaV1.5 and SERCA2 protein levels did not differ between control and VPC rabbits. Our results showed that ionic

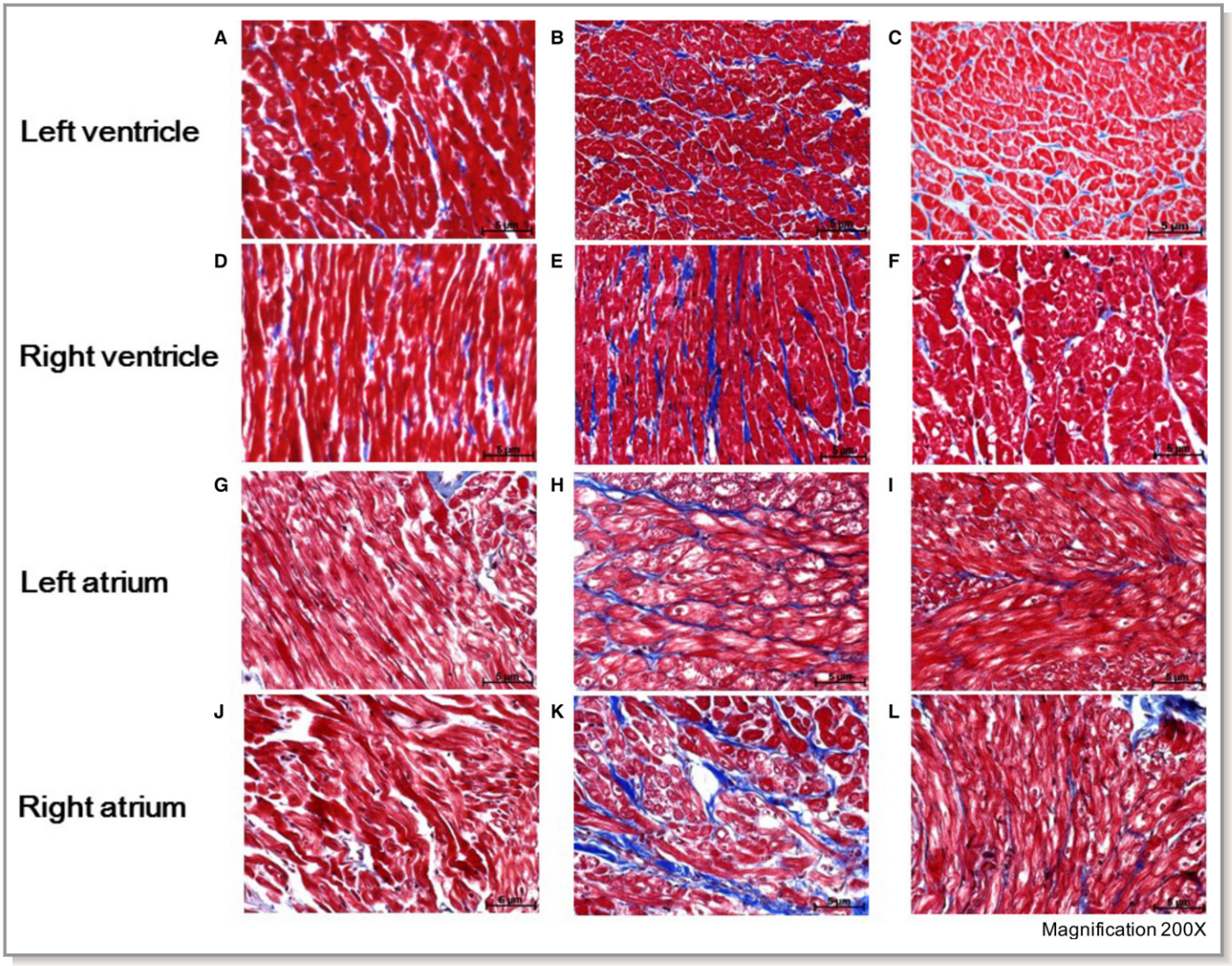

Figure 5. Ventricular and atrial tissue fibrosis detected with Masson's trichrome staining among all groups. A, Control rabbits left ventricle; (B) VPC rabbits left ventricle; (C) VPC-RDN rabbits left ventricle; (D) control rabbits right ventricle; (E) VPC rabbits right ventricle; (F) VPC-RDN rabbits right ventricle; (G) control rabbits left atrium; (H) VPC rabbits left atrium; (I) VPC-RDN rabbits left atrium; (J) control rabbits right atrium; (K) VPC rabbits right atrium; and (L) VPC-RDN rabbits right atrium. Blue color represents the collagen component, whereas the red color is the normal ventricular or atrial myocardium. RDN indicates renal artery sympathetic denervation; VPC, ventricular premature complex.

channel remodeling did not happen in VPC-induced cardiomyopathy.

Mechanism of VPC-Induced Cardiomyopathy

The mechanisms of the development of dilated cardiomyopathy induced by frequent VPCs have not been clarified. One possible mechanism of them is the LV mechanical alterations. The irregular beats of frequent VPCs lead to an LV mechanical dyssynchrony, which can contribute to the increase of the LV filling pressures and atrial overload.[26,27] As a result, those hemodynamic changes activate the renin-angiotensin-aldosterone system in ventricle and atria through stretch of the heart and inflammatory cytokines, which might be associated with the progression of cardiac remodeling and finally lead to heart failure.[4,28–30] We speculate that ventricular chamber dilatation and myocardial fibrosis are the consequence from those pathological influences.

In heart failure, cardiac sympathetic activity is initially increased.[31] The level of sympathetic nerve activity was evaluated by the measurement of norepinephrine spillover, and it was shown that the increase in cardiac norepinephrine spillover occurred at an earlier stage of heart failure than it does to the kidney.[32,33] On the other hand, as the development of heart failure, it was reported that myocardial norepinephrine and cardiac TH activity were decreased.[31,34,35] In the present study, cardiac sympathetic nerve activity was increased in VPC rabbits compared to control, but renal catecholamine levels in

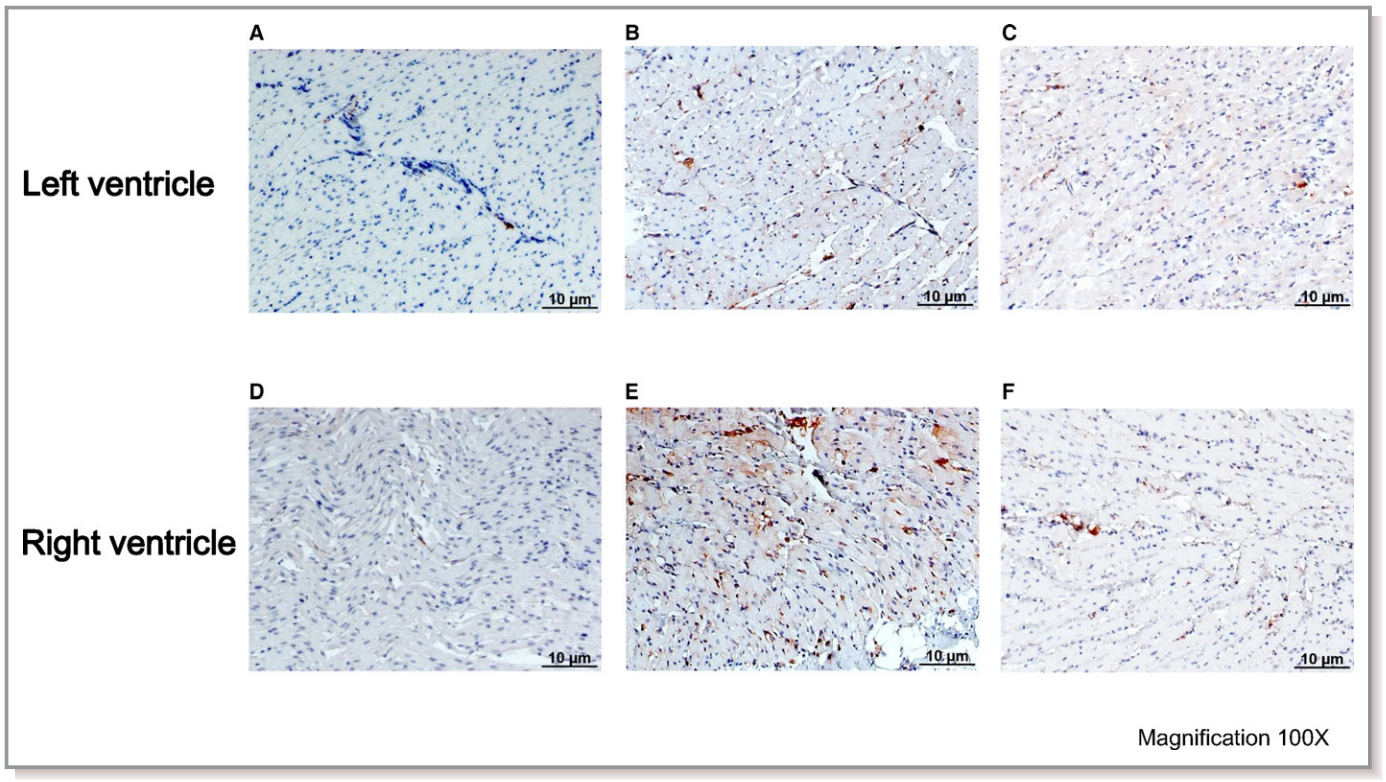

Figure 6. Immunohistochemistry staining in the ventricle. A, control rabbits left ventricle; (B) VPC rabbits left ventricle; (C) VPC-RDN rabbits left ventricle; (D) control rabbits right ventricle; (E) VPC rabbits right ventricle; and (F) VPC-RDN rabbits right ventricle. Tyrosine hydroxylase staining in biventricle showing increased sympathetic innervation in VPC rabbits compared with control rabbits and VPC-RDN rabbits. RDN indicates renal artery sympathetic denervation; VPC, ventricular premature complex.

these groups were similar. Therefore, our study models might be at an early stage of the development of VPC-induced cardiomyopathy, and RDN may only be helpful in milder forms of VPC-induced cardiomyopathy.

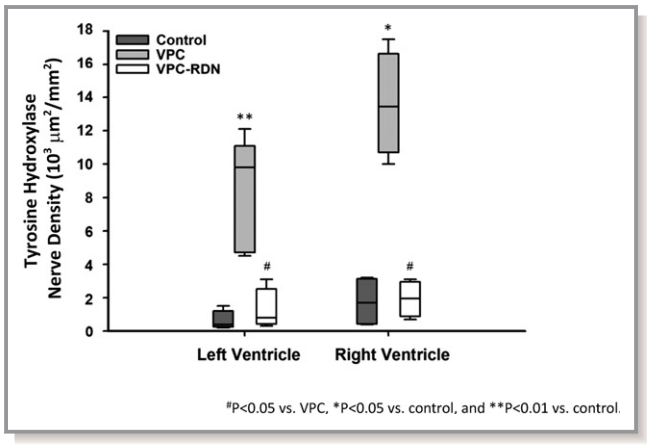

Figure 7. Cardiac sympathetic activity in the ventricle from 3 groups. Sympathetic neuron marker densities in left ventricle and right ventricle were significantly higher in VPC rabbits compared with those of control and VPC-RDN rabbits, respectively. RDN indicates renal artery sympathetic denervation; VPC, ventricular premature complex.

Effect of RDN on Ventricular Tachyarrhythmia

Increases in the renin-angiotensin-aldosterone system and sympathetic activity are known to be associated with promotion of ventricular arrhythmogenic substrate and the genesis of ventricular arrhythmia.[14,36] Therefore, RDN may be an effective therapy for management of ventricular arrhythmia because RDN can regulate renin-angiotensin-aldosterone system activation and sympathetic activity.[14,15] Our study demonstrated that VF inducibility was higher in VPC rabbits than that in control rabbits. Cardiac sympathetic nerve activity was increased in VPC rabbits compared to control, but this activity was suppressed in VPC-RDN rabbits. In VPC rabbits, renin after pacing was significantly higher than that of baseline. On the other hand, in VPC-RDN rabbits, there were no significant differences in renin between baseline and after pacing. It is generally considered that activity of the renin-angiotensine-aldosterone system affects cardiac fibrosis, inflammation, and apoptosis.[24,37] Recently, it was demonstrated that pharmacological renin inhibition or genetic deletion of angiotensin type 1a receptor suppressed cardiac fibrosis and reduced the incidence of ventricular arrhythmia.[36] Their results support that RDN inhibited the development of cardiac fibrosis and decreased VF inducibility.

In the present study, ventricular and atrial structural remodeling were induced by frequent VPCs. Literature has demonstrated that β-blocker therapy and radiofrequency catheter ablation may be preferable for VPC suppression.[6,7,38] From this study, RDN might be an alternative therapeutic strategy in selected patients, particularly when β-blocker therapy and radiofrequency catheter ablation have been ineffective or not tolerated.

Limitations

Our sample size was small and the follow-up period was limited. However, our study did demonstrate that 50% VPC burden during a 5-week follow-up induced ventricular chamber dilatation and RDN suppressed the development of ventricular structural change. We would consider performing a study in the future to investigate whether RDN leads to beneficial ventricular remodeling in VPC-induced cardiomyopathy at the late stage.

Conclusion

Frequent VPCs lead to the development of structural remodeling and high VF inducibility. RDN prevents the remodeling process through antifibrosis, supporting that reverse structural remodeling is a pivotal mechanism of RDN in the protection of the heart from frequent VPC-induced cardiomyopathy.

Acknowledgments

We thank the Clinical Research Core Laboratory of Taipei Veterans General Hospital for providing experimental space and facilities.

Sources of Funding

The present work was supported by the Taipei Veterans General Hospital (V102B-002, V102E7-003, V103C-042, V103C-126, V103E7-002, VGHUST103-G1-3-1, V104C-131, and V104E7-003), Ministry of Science and Technology (NSC 102-2325-B-010-005, MOST 103-2314-B-075-062-MY3, and MOST 104-2314-B-075-065-MY2), and Research Foundation of Cardiovascular Medicine (RFCM 101-01-001 and 104-01-009-1).

Disclosures

None.

References

1. Simpson RJ Jr, Cascio WE, Schreiner PJ, Crow RS, Rautaharju PM, Heiss G. Prevalence of premature ventricular contractions in a population of African American and white men and women: the Atherosclerosis Risk in Communities (ARIC) study. *Am Heart J*. 2002;143:535–540.
2. Messineo FC. Ventricular ectopic activity: prevalence and risk. *Am J Cardiol*. 1989;64:53J–56J.
3. Haïssaguerre M, Derval N, Sacher F, Jesel L, Deisenhofer I, de Roy L, Pasquié JL, Nogami A, Babuty D, Yli-Mayry S, De Chillou C, Scanu P, Mabo P, Matsuo S, Probst V, Le Scouarnec S, Defaye P, Schlaepfer J, Rostock T, Lacroix D, Lamaison D, Lavergne T, Aizawa Y, Englund A, Anselme F, O'Neill M, Hocini M, Lim KT, Knecht S, Veenhuyzen GD, Bordachar P, Chauvin M, Jais P, Coureau G, Chene G, Klein GJ, Clémenty J. Sudden cardiac arrest associated with early repolarization. *N Engl J Med*. 2008;358:2016–2023.
4. Lee GK, Klarich KW, Grogan M, Cha YM. Premature ventricular contraction-induced cardiomyopathy: a treatable condition. *Circ Arrhythm Electrophysiol*. 2012;5:229–236.
5. Tanaka Y, Rahmutula D, Duggirala S, Nazer B, Fang Q, Olgin J, Sievers R, Gerstenfeld EP. Diffuse fibrosis leads to a decrease in unipolar voltage: validation in a swine model of premature ventricular contraction-induced cardiomyopathy. *Heart Rhythm*. 2016;13:547–554.
6. Yarlagadda RK, Iwai S, Stein KM, Markowitz SM, Shah BK, Cheung JW, Tan V, Lerman BB, Mittal S. Reversal of cardiomyopathy in patients with repetitive monomorphic ventricular ectopy originating from the right ventricular outflow tract. *Circulation*. 2005;112:1092–1097.
7. Bogun F, Crawford T, Reich S, Koelling TM, Armstrong W, Good E, Jongnarangsin K, Marine JE, Chugh A, Pelosi F, Oral H, Morady F. Radiofrequency ablation of frequent, idiopathic premature ventricular complexes: comparison with a control group without intervention. *Heart Rhythm*. 2007;4:863–867.
8. Huizar JF, Kaszala K, Potfay J, Minisi AJ, Lesnefsky EJ, Abbate A, Mezzaroma E, Chen Q, Kukreja RC, Hoke NN, Thacker LR II, Ellenbogen KA, Wood MA. Left ventricular systolic dysfunction induced by ventricular ectopy: a novel model for premature ventricular contraction- induced cardiomyopathy. *Circ Arrhythm Electrophysiol*. 2011;4:543–549.
9. Deyell MW, Park KM, Han Y, Frankel DS, Dixit S, Cooper JM, Hutchinson MD, Lin D, Garcia F, Bala R, Riley MP, Gerstenfeld E, Callans DJ, Marchlinski FE. Predictors of recovery of left ventricular dysfunction after ablation of frequent ventricular premature depolarizations. *Heart Rhythm*. 2012;9:1465–1472.
10. van Brussel PM, Lieve KV, de Winter RJ, Wilde AA. Cardiorenal axis and arrhythmias: will renal sympathetic denervation provide additive value to the therapeutic arsenal? *Heart Rhythm*. 2015;12:1080–1087.
11. Bhatt DL, Kandzari DE, O'Neill WW, D'Agostino R, Flack JM, Katzen BT, Leon MB, Liu M, Mauri L, Negoita M, Cohen SA, Oparil S, Rocha-Singh K, Townsend RR, Bakris GL; SYMPLICITY HTN-3 Investigators. A controlled trial of renal denervation for resistant hypertension. *N Engl J Med*. 2014;370:1393–1401.
12. Böhm M, Ewen S, Kindermann I, Linz D, Ukena C, Mahfoud F. Renal denervation and heart failure. *Eur J Heart Fail*. 2014;16:608–613.
13. Pokushalov E, Romanov A, Katritsis DG, Artyomenko S, Bayramova S, Losik D, Baranova V, Karaskov A, Steinberg JS. Renal denervation for improving outcomes of catheter ablation in patients with atrial fibrillation and hypertension: early experience. *Heart Rhythm*. 2014;11:1131–1138.
14. Huang B, Scherlag BJ, Yu L, Lu Z, He B, Jiang H. Renal sympathetic denervation for treatment of ventricular arrhythmias: a review on current experimental and clinical findings. *Clin Res Cardiol*. 2015;104:535–543.
15. Wang X, Zhao Q, Huang H, Tang Y, Xiao J, Dai Z, Yu S, Huang C. Effect of renal sympathetic denervation on atrial substrate remodeling in ambulatory canines with prolonged atrial pacing. *PLoS One*. 2013;8:e64611.
16. Linz D, Wirth K, Ukena C, Mahfoud F, Pöss J, Linz B, Böhm M, Neuberger HR. Renal denervation suppresses ventricular arrhythmias during acute ventricular ischemia in pigs. *Heart Rhythm*. 2013;10:1525–1530.
17. Ng GA, Brack KE, Patel VH, Coote JH. Autonomic modulation of electrical restitution, alternans and ventricular fibrillation initiation in the isolated heart. *Cardiovasc Res*. 2007;73:750–760.
18. Ng GA, Mantravadi R, Walker WH, Ortin WG, Choi BR, de Groat W, Salama G. Sympathetic nerve stimulation produces spatial heterogeneities of action potential restitution. *Heart Rhythm*. 2009;6:696–706.
19. Huang B, Yu L, He B, Lu Z, Wang S, He W, Yang K, Liao K, Zhang L, Jiang H. Renal sympathetic denervation modulates ventricular electrophysiology and has a protective effect on ischemia-induced ventricular arhythmia. *Exp Physiol*. 2014;99:1467–1477.
20. Pogwizd SM, Schlotthauer K, Li L, Yuan W, Bers DM. Arrhythmogenesis and contractile dysfunction in heart failure: roles of sodium-calcium exchange, inward rectifier potassium current, and residual beta-adrenergic responsiveness. *Circ Res*. 2001;88:1159–1167.
21. Valdivia CR, Chu WW, Pu J, Foell JD, Haworth RA, Wolff MR, Kamp TJ, Makielski JC. Increased late sodium current in myocytes from a canine heart failure model and from failing human heart. *J Mol Cell Cardiol*. 2005;38:475–483.

22. Pitt GS, Dun W, Boyden PA. Remodeled cardiac calcium channels. *J Mol Cell Cardiol*. 2006;41:373–388.
23. Hasenfuss G, Pieske B. Calcium cycling in congestive heart failure. *J Mol Cell Cardiol*. 2002;34:951–969.
24. Dohi Y, Ohashi M, Sugiyama M, Takase H, Sato K, Ueda R. Candesartan reduces oxidative stress and inflammation in patients with essential hypertension. *Hypertens Res*. 2003;26:691–697.
25. Wang Y, Eltit JM, Kaszala K, Tan A, Jiang M, Zhang M, Tseng GN, Huizar JF. Cellular mechanism of premature ventricular contraction-induced cardiomyopathy. *Heart Rhythm*. 2014;11:2064–2072.
26. Park Y, Kim S, Shin J, Oh AR, Shin EJ, Lee JH, Ahn T, Cha JY, Moon J. Frequent premature ventricular complex is associated with left atrial enlargement in patients with normal left ventricular ejection fraction. *Pacing Clin Electrophysiol*. 2014;37:1455–1461.
27. Wang J, Kurrelmeyer KM, Torre-Amione G, Nagueh SF. Systolic and diastolic dyssynchrony in patients with diastolic heart failure and the effect of medical therapy. *J Am Coll Cardiol*. 2007;49:88–96.
28. Nakashima H, Kumagai K, Urata H, Gondo N, Ideishi M, Arakawa K. Angiotensin II antagonist prevents electrical remodeling in atrial fibrillation. *Circulation*. 2000;101:2612–2617.
29. Kumagai K, Nakashima H, Urata H, Gondo N, Arakawa K, Saku K. Effects of angiotensin II type 1 receptor antagonist on electrical and structural remodeling in atrial fibrillation. *J Am Coll Cardiol*. 2003;41:2197–2204.
30. Chen T, Koene R, Benditt DG, Lü F. Ventricular ectopy in patients with left ventricular dysfunction: should it be treated? *J Card Fail*. 2013;19:40–49.
31. Triposkiadis F, Karayannis G, Giamouzis G, Skoularigis J, Louridas G, Butler J. The sympathetic nervous system in heart failure physiology, pathophysiology, and clinical implications. *J Am Coll Cardiol*. 2009;54:1747–1762.
32. Esler M, Kaye D, Lambert G, Esler D, Jennings G. Adrenergic nervous system in heart failure. *Am J Cardiol*. 1997;80:7L–14L.
33. Esler M, Jennings G, Korner P, Willett I, Dudley F, Hasking G, Anderson W, Lambert G. Assessment of human sympathetic nervous system activity from measurements of norepinephrine turnover. *Hypertension*. 1988;11:3–20.
34. Kawai H, Mohan A, Hagen J, Dong E, Armstrong J, Stevens SY, Liang CS. Alterations in cardiac adrenergic terminal function and beta-adrenoceptor density in pacing-induced heart failure. *Am J Physiol Heart Circ Physiol*. 2000;278:H1708–H1716.
35. Liang CS, Yatani A, Himura Y, Kashiki M, Stevens SY. Desipramine attenuates loss of cardiac sympathetic neurotransmitters produced by congestive heart failure and norepinephrine infusion. *Am J Physiol Heart Circ Physiol*. 2003;284:H1729–H1736.
36. Yamada C, Kuwahara K, Yamazaki M, Nakagawa Y, Nishikimi T, Kinoshita H, Kuwabara Y, Minami T, Yamada Y, Shibata J, Nakao K, Cho K, Arai Y, Honjo H, Kamiya K, Nakao K, Kimura T. The renin-angiotensin system promotes arrhythmogenic substrates and lethal arrhythmias in mice with non-ischaemic cardiomyopathy. *Cardiovasc Res*. 2016;109:162–173.
37. Nickenig G, Harrison DG. The AT(1)-type angiotensin receptor in oxidative stress and atherogenesis: part I: oxidative stress and atherogenesis. *Circulation*. 2002;105:393–396.
38. Krittayaphong R, Bhuripanyo K, Punlee K, Kangkagate C, Chaithiraphan S. Effect of atenolol on symptomatic ventricular arrhythmia without structural heart disease: a randomized placebo-controlled study. *Am Heart J*. 2002;144:e10.